

# Voltage-induced singularities in transport through molecular junctions

O. Entin-Wohlman,<sup>1,2,\*</sup> Y. Imry,<sup>3</sup> and A. Aharony<sup>4,†</sup>

<sup>1</sup>*Department of Physics, Ben Gurion University, Beer Sheva 84105, Israel*

<sup>2</sup>*Albert Einstein Minerva Center for Theoretical Physics,  
Weizmann Institute of Science, Rehovot 76100, Israel*

<sup>3</sup>*Department of Condensed Matter Physics, Weizmann Institute of Science, Rehovot 76100, Israel*

<sup>4</sup>*Department of Physics and the Ilse Katz Center for Meso- and Nano-Scale Science and Technology,  
Ben Gurion University, Beer Sheva 84105, Israel*

(Dated: March 9, 2021)

The inelastic scattering of electrons which carry current through a single-molecule junction is modeled by a quantum dot, coupled to electron reservoirs via two leads. When the electron is on the dot, it is coupled to a single harmonic oscillator of frequency  $\omega_0$ . At zero temperature, the resonance peak in the linear-response conductance always narrows down due to the coupling with the vibrational mode. However, this narrowing down is given by the Franck-Condon factor only for narrow resonances. Contrary to some claims in the literature, the linear-response conductance does not exhibit any side-bands at zero temperature. Small side-bands, of order  $\exp[-\beta\hbar\omega_0]$ , do arise at finite temperatures. The single-particle density of states exhibits discontinuities and logarithmic singularities at the frequencies corresponding to the opening of the inelastic channels, due to the imaginary and real parts of the self-energy. The same singularities also generate discontinuities and logarithmic divergences in the differential conductance at and around the inelastic thresholds. These discontinuities usually involve upwards steps, but these steps become negative within a rather narrow range of the elastic transparency of the junction. This range shrinks further as the the excitation energy exceeds the bare resonance width.

PACS numbers: 71.38.-k,73.63.Kv,73.21.La

Keywords: electron-vibration interaction, transport through molecules and quantum dots, channel opening, Franck-Condon factors, Kramers-Kronig relations

## I. INTRODUCTION

Single-molecule junctions based on direct bonding of a small molecule between two metallic electrodes seem by now rather established experimentally.<sup>1,2,3,4,5,6,7,8,9</sup> The electronic transport through such a molecular bridge is attracting a great deal of interest, including the invention of ingenious experimental realizations for it (see, for example, the recent Refs. 10). Besides the possible technological advantages of “molecular electronics”,<sup>11</sup> there are many issues that make this problem of great interest from both the basic science and the application points of view. The possibility of directly addressing a *single* microscopic quantum system with an ordinary measurement apparatus should shed light on fundamental quantum measurement questions.

Electrons passing through the small molecule may change its quantum state (electronic, vibrational, and in certain cases also rotational, and even the conformation<sup>12</sup> of the molecule). These may require a finite energy transfer from the transport electron. Thus, the dynamics of the molecule may create interesting structures in the I-V characteristics.<sup>13,14</sup> These rich characteristics, resembling the one observed in inelastic electron tunneling spectroscopy (IETS),<sup>15</sup> depend on important experimental details such as the equilibration time of the vibrations compared to the typical time between consecutive electrons passing through the junction, or whether the electrons can pump the molecule into higher vibrational states. Such measurements provide a handle on study-

ing molecular properties and their modifications by the binding to the electrodes. In some cases they may also help to identify the molecule which has been bound in the bridge.

The configurational modification of the molecule by the tunneling electron is usually described by a linear coupling of the electron with e.g. the vibrational modes, while the oscillating location of the whole molecule is modeled by the dependence of the tunneling matrix elements to the leads on the vibrational degrees of freedom.<sup>16</sup> As is well-known, one may eliminate the linear electron-phonon interaction by a canonical transformation which dresses the tunneling matrix elements by the phonon cloud (the Holstein polaron).<sup>17</sup> The resulting matrix elements contain the Franck-Condon factors. These tend to block the conductance at off-resonant situations (the Franck-Condon blockade).<sup>18,19</sup> However, the top of the resonance conductance is not reduced by these factors.<sup>16</sup> Indeed, we find that the coupling to the vibrational mode causes a narrowing of the resonance. This narrowing is described by the ‘usual’ Franck-Condon blockade only in the limit of very narrow ‘bare’ resonances, namely very long dwell times of the electrons on the resonances. We find that reducing this dwell time weakens the Franck-Condon blocking.

Transport through small molecules offers new means of studying tunneling of electrons interacting with vibrational modes. Theoretical studies of the coupling between molecular vibrations and electronic states participating in the tunneling have begun with the exact calcu-

lation of the single-electron transmission, in which the presence of the Fermi seas representing the leads has been essentially ignored.<sup>20,21</sup> The single-electron transmission naturally exhibits resonances at energies corresponding to the vibration frequencies (these are often called “side-bands”). Such side-bands also appear in the local (on-molecule) single-particle density of states, computed in the presence of the leads.<sup>22,23</sup> There are claims in the literature<sup>24,25</sup> that these side-bands are reflected in, for example, the gate-potential dependence of the linear-response conductance. However, as has been emphasized by Mitra *et al.*<sup>16</sup> and discussed in detail below, such side-bands cannot appear at zero temperature in the linear-response regime. We shall demonstrate their appearance, albeit weakly, at finite temperatures.

Indeed, an electron crossing the molecular bridge may do so inelastically or elastically (with or without changing the excitation state of the molecule). In the former case the electron will lose its phase coherence – a problem to which we will return in future work (see the discussion in Ref. 26). Here, we concentrate on the structure of the conductance as a function of the bias voltage  $V$  and the gate potential, represented by the electrochemical potential  $\mu$  (when applying the latter is feasible). Clearly, at low temperatures only elastic processes and inelastic ones *exciting* the molecule are possible. The latter can happen only if the transmitted electron can supply the energy required for the molecular excitation. Focussing on a molecular vibration of frequency  $\omega_0$ , it is clear, then, that it can be excited only when the bias voltage  $V$  exceeds  $\hbar\omega_0/e$ , namely, beyond the linear-response regime. This<sup>16</sup> will be confirmed by the detailed calculations below.

The footprints of the inelastic processes appear in the differential conductance when plotted as a function of the bias voltage. (For analyses of the full counting statistics of a vibrating junction, see Refs. 27.) This regime has been studied experimentally rather intensively. Theoretically, it has been treated by employing a variety of methods and numerical techniques.<sup>28,29,30,31,32</sup> At low temperatures, the inelastic channel comes in when the bias voltage exceeds  $\hbar\omega_0/e$ . This however does not necessarily imply an increase of the total conductance, since the elastic conduction channel might be modified as well. Indeed, interestingly enough, it has been observed that the “step” in the conductance at  $V = \hbar\omega_0/e$  appears either as a decrease or an increase in the differential conductance.<sup>3,7,8,9,10</sup> Theoretical work addressing this issue<sup>33,34</sup> claimed that this behavior depends in a universal manner on the bare elastic transparency of the junction,  $\mathcal{T}$ , such that the differential conductance steps upwards when  $\mathcal{T} < 1/2$ , and downwards when  $\mathcal{T} > 1/2$ . This claim has been refuted recently in a seminal paper by Egger and Gogolin.<sup>35</sup> We confirm their conclusion. Moreover, we find that the conductance steps downwards only in a narrow range of  $\mathcal{T}$ , which becomes narrower as the ratio of the excitation energy  $\hbar\omega_0$  to the bare resonance width  $\Gamma_0$  increases.

Another important aspect concerns the instabilities in the vibration modes possibly induced by the current.<sup>16,36,37</sup> In particular, Ref. 37 points out the inapplicability of the perturbation theory in the electron-vibration coupling once the nonequilibrium regime is reached. We show below that the step-like structure in the differential conductance at  $V = \hbar\omega_0/e$  implies another type of breakdown of the perturbation theory. It turns out that the opening of the inelastic channel is inevitably accompanied by the appearance of *logarithmic singularities* at the same bias voltage. Those are forced via the Kramers-Kronig relations and are related to the singularities found by Engelsberg and Schrieffer<sup>38</sup> for bulk Einstein phonons. In this way we confirm the important (and seemingly, un-noticed) result of Mitra *et al.*<sup>16</sup> and Egger and Gogolin<sup>35</sup>: beside the step-like structure, caused by the inelastic tunneling processes, the differential conductance develops a logarithmic singularity (at zero temperature, and to second order in the electron-vibration coupling) as the bias voltage crosses the vibration energy. Near the threshold voltage  $V = \hbar\omega_0/e$ , that singularity dominates the differential conductance.

It thus seems that there are several relevant issues in the theory of transport through a vibrating junction which are either still under debate or are not entirely clear. These concern the existence of side-bands, the dependence of the conductance on the junction transparency, the structure of the differential conductance near the opening of the inelastic channel, and the precise effect of the Franck-Condon factors on the resonances, including what happens when the resonance width exceeds the vibration frequency. Below, we give our answers to these questions and provide further physical interpretations for them. In order not to obscure the basic physics by lengthy computations, we restrict ourselves to the simplest model, of a single resonance connected symmetrically to two leads and coupled linearly to a vibration. In addition, we apply lowest-order perturbation theory in the electron-vibration coupling. We believe that a complete analytical discussion of the outcome of this model will shed further light on the intriguing non-equilibrium behavior of the vibration-induced conductance.

Section II gives the Hamiltonian, and then expresses the current through the system in terms of the Green functions, which contain the contributions from the coupling to the vibrational mode. The detailed calculation of these Green functions is described in the Appendix. Section III presents the results for the conductance and for the density of states in the linear-response regime, while Sec. IV discusses the differential conductance at finite bias voltage (but zero temperature). Finally, we detail our conclusions in Sec. V.

## II. THE MODEL

We consider the differential conductance of a small system, consisting of two leads connected together via a

“dot”. The two leads are assumed to be identical, except for being attached to reservoirs held at possibly different chemical potentials,  $\mu_L \equiv \mu + eV/2$  and  $\mu_R \equiv \mu - eV/2$ . When the electron is on the dot, it is coupled to a single harmonic oscillator of frequency  $\omega_0$ . The Hamiltonian of this system is

$$\mathcal{H} = \mathcal{H}_{\text{lead}} + \mathcal{H}_{\text{dot}} + \mathcal{H}_{\text{coup}}. \quad (1)$$

The lead Hamiltonian is [using  $k(p)$  for the left (right) lead, with the same lattice constant  $a = 1$ ]

$$\mathcal{H}_{\text{lead}} = \sum_k \epsilon_k c_k^\dagger c_k + \sum_p \epsilon_p c_p^\dagger c_p, \quad (2)$$

with

$$\epsilon_{k(p)} = -2J \cos k(p). \quad (3)$$

The Hamiltonian of the dot is

$$\mathcal{H}_{\text{dot}} = \epsilon_0 c_0^\dagger c_0 + \hbar\omega_0 (b^\dagger b + \frac{1}{2}) + \gamma (b + b^\dagger) c_0^\dagger c_0, \quad (4)$$

where  $\epsilon_0$  is the energy level on the dot, and  $\gamma$  is the coupling energy of the electron (while it resides on the dot) with the oscillator. Below we often set  $\hbar = 1$ . Finally, the coupling between the dot and the leads is described by

$$\mathcal{H}_{\text{coup}} = \sum_k V_k (c_k^\dagger c_0 + \text{hc}) + \sum_p V_p (c_p^\dagger c_0 + \text{hc}), \quad (5)$$

with

$$V_{k(p)} = -\sqrt{\frac{2}{N}} J_0 \sin k(p). \quad (6)$$

(The wave functions on the leads are normalized assuming that each lead consists of  $N$  sites.) In Eqs. (3) and (6),  $J$  is the overlap amplitude along the leads and  $J_0$  is the overlap amplitude between the leads and the dot (taken to be symmetric, for simplicity), all in units of energy. The operators  $c_0^\dagger$ ,  $c_k^\dagger$ , and  $c_p^\dagger$  ( $c_0$ ,  $c_k$ , and  $c_p$ ) create (annihilate) an electron on the dot, on the left lead, and on the right lead, respectively, while  $b^\dagger$  ( $b$ ) creates (annihilates) an excitation of the harmonic oscillator, of frequency  $\omega_0$ . This model system has gained much theoretical interest before, see for example Refs. 16, 18, 19, 20, 21, 22, 24, 25, 29, 31 and 35.

### A. The currents in the system

The currents flowing in this system can be expressed in terms of the Keldysh Green functions: those on the dot are marked by the subscript 00, and the mixed ones are marked by the subscripts  $k(p)0$ , see Appendix A for

details. The current entering the dot from the left lead,  $I_{LD}$ , is

$$\begin{aligned} I_{LD} &= e \int \frac{d\omega}{2\pi} \sum_k V_k [G_{k0}^<(\omega) - G_{0k}^<(\omega)] \\ &= ie \int \frac{d\omega}{2\pi} \Gamma_0(\omega) \\ &\quad \times \left( -G_{00}^<(\omega) + f_L(\omega) [G_{00}^a(\omega) - G_{00}^r(\omega)] \right), \quad (7) \end{aligned}$$

and that from the right one,  $I_{RD}$ , is

$$\begin{aligned} I_{RD} &= e \int \frac{d\omega}{2\pi} \sum_p V_p [G_{p0}^<(\omega) - G_{0p}^<(\omega)] \\ &= ie \int \frac{d\omega}{2\pi} \Gamma_0(\omega) \\ &\quad \times \left( -G_{00}^<(\omega) + f_R(\omega) [G_{00}^a(\omega) - G_{00}^r(\omega)] \right). \quad (8) \end{aligned}$$

In Eqs. (7) and (8),  $f_{L,R}(\omega) = 1/[e^{\beta(\omega - \mu_{L,R})} + 1]$  are the Fermi distributions in the two reservoirs, and  $\Gamma_0$  is the imaginary part of the self-energy  $\Sigma_0$  due to the coupling with the leads, Eqs. (A11) and (A35). Obviously, current conservation requires  $I_{LD} + I_{RD}$  to vanish. Indeed, upon adding Eqs. (7) and (8) [and employing Eqs. (A12) and (A35)] we find that current is conserved. Hence, the net current  $I$  can be obtained as the difference between the two currents,  $I_{LD}$  and  $I_{RD}$ . This leads to

$$I = e \int \frac{d\omega}{2\pi} \Gamma_0(\omega) [f_L(\omega) - f_R(\omega)] \text{Im} G_{00}^a(\omega). \quad (9)$$

This well-known exact result in which the local density of states on the dot,  $\text{Im} G_{00}^a(\omega)$ , contains all of its dynamics, including the coupling to the oscillator, is similar to the result as given, e.g., in Refs. 16, 22, 24, 35 and 39. It is customary to use the expression (9) also for nonlinear transport. We remark that this is valid only for bias voltages that are not too large.<sup>40</sup> Equation (9) neglects the effects of the finite field on the system, such as the nonlinear screening, the induced changes in  $\epsilon_0$  and  $J_0$ , and the possibility, mentioned above, of “pumping” the molecule into higher states. *Only when all the above finite-voltage corrections are neglected, does the Keldysh formulation justify using this result also in the nonlinear regime.*

The coupling with the harmonic oscillator affects the dot Green functions,  $G_{00}^a$  and  $G_{00}^r$ . In the absence of the coupling to the vibrations, the ‘bare’ dot Green function is given by

$$\mathcal{G}_{00}^r = \frac{1}{\omega - \epsilon_0 - \Sigma_0^r}. \quad (10)$$

Neglecting the frequency dependence of the self-energy due to the coupling with the leads,  $\Sigma_0$ , (this is the “wide-band approximation”) and absorbing  $\text{Re}\Sigma_0$  into  $\epsilon_0$ , i.e.,  $\epsilon_0 \rightarrow \epsilon_{\text{res}} = \epsilon_0 + \text{Re}\Sigma_0$ , the zeroth-order Green function,

Eq. (10), becomes

$$\mathcal{G}_{00}^r(\omega) = \frac{1}{\omega - \epsilon_{\text{res}} + i\Gamma_0}. \quad (11)$$

Expanding the Green function up to order  $\gamma^2$  yields

$$G_{00}^a = \mathcal{G}_{00}^a + (\mathcal{G}_{00}^a)^2 (\Delta\epsilon_0 + \Sigma_{\text{ho}}^a) \quad (12)$$

$$= \mathcal{G}_{00}^a + (\mathcal{G}_{00}^a)^2 (\Delta E \pm i\text{Im}\Sigma_{\text{ho}}^a), \quad (13)$$

where  $\Sigma_{\text{ho}}$  is the self-energy due to the coupling to the oscillator,  $\Delta\epsilon_0$  is the shift of the energy, Eqs. (A15) and (A27),

$$\Delta\epsilon_0 = -\frac{2\gamma^2}{\omega_0} \int \frac{d\omega}{2\pi} |\mathcal{G}_{00}^r(\omega)|^2 \Gamma_0(\omega) [f_L(\omega) + f_R(\omega)], \quad (14)$$

and we have defined  $\Delta E = \Delta\epsilon_0 + \text{Re}\Sigma_{\text{ho}}^a$ .

From the expansion Eq. (13) it follows that the current can be written in the form<sup>41</sup>

$$I = I_0 + I_{\text{co}} + I_{\text{inco}}, \quad (15)$$

where  $I_0$  is the current in the absence of the coupling with the oscillator,

$$I_0 = e \int \frac{d\omega}{2\pi} \Gamma_0(\omega) [f_L(\omega) - f_R(\omega)] \text{Im}\mathcal{G}_{00}^a(\omega), \quad (16)$$

$I_{\text{co}}$  is the current involving the (real) shift in the resonant level (which depends on the frequency and the chemical potentials),

$$I_{\text{co}} = -ie \int \frac{d\omega}{4\pi} \Gamma_0(\omega) [f_L(\omega) - f_R(\omega)] \times [(\mathcal{G}_{00}^a(\omega))^2 - (\mathcal{G}_{00}^r(\omega))^2] \Delta E, \quad (17)$$

and  $I_{\text{inco}}$  is the current involving the imaginary part of  $\Sigma_{\text{ho}}$ ,

$$I_{\text{inco}} = e \int \frac{d\omega}{4\pi} \Gamma_0(\omega) [f_L(\omega) - f_R(\omega)] \times [(\mathcal{G}_{00}^a(\omega))^2 + (\mathcal{G}_{00}^r(\omega))^2] \text{Im}\Sigma_{\text{ho}}^a(\omega). \quad (18)$$

Below we mainly consider zero temperature. (The effects of a finite temperature on the linear-response conductance are considered in Sec. III C.) Furthermore, we ignore the explicit dependence of  $\Gamma_0$  on  $\omega$ . At zero temperature, the zeroth-order current is

$$I_0 = \frac{e}{2\pi} \int_{\mu_R}^{\mu_L} d\omega \frac{\Gamma_0^2}{\omega^2 + \Gamma_0^2} = \frac{e\Gamma_0}{2\pi} \left( \arctan \frac{\mu_L}{\Gamma_0} - \arctan \frac{\mu_R}{\Gamma_0} \right), \quad (19)$$

the current due to the effective shift in the resonance energy, Eq. (17), is [see Eq. (11)]

$$I_{\text{co}} = \frac{e\Gamma_0^2}{\pi} \int_{\mu_R}^{\mu_L} d\omega \frac{\omega}{(\omega^2 + \Gamma_0^2)^2} \Delta E(\omega, \mu_L, \mu_R) \equiv \frac{e\Gamma_0^2}{\pi} \int_{\mu_R}^{\mu_L} d\omega \frac{\omega}{(\omega^2 + \Gamma_0^2)^2} (\Delta\epsilon_0(\mu_L, \mu_R) + \text{Re}\Sigma_{\text{ho}}^a(\omega, \mu_L, \mu_R)), \quad (20)$$

and the current due to the imaginary part of the self-energy, Eq. (18), is

$$I_{\text{inco}} = \frac{e\Gamma_0}{2\pi} \int_{\mu_R}^{\mu_L} d\omega \frac{\omega^2 - \Gamma_0^2}{(\omega^2 + \Gamma_0^2)^2} \text{Im}\Sigma_{\text{ho}}^a(\omega, \mu_L, \mu_R). \quad (21)$$

## B. The zero temperature Green functions and self-energies

The detailed calculations of the contributions to the Green functions due to the coupling with the oscillator are given in the Appendix. At zero temperature, Eq. (14) becomes

$$\Delta\epsilon_0 = -\frac{\gamma^2\Gamma_0}{\pi\omega_0} \left( \int^{\mu_L} + \int^{\mu_R} \right) \frac{d\omega}{(\omega - \epsilon_{\text{res}})^2 + \Gamma_0^2}. \quad (22)$$

(It seems that this shift was overlooked in Ref. 35.) In computing the explicit expressions of the currents and the conductances [see Secs. III and IV], it is expedient<sup>35</sup> to measure the frequencies  $\omega$  and  $\omega'$ , as well as the chemical potentials  $\mu_{L(R)}$  from  $\epsilon_{\text{res}}$ . We then find

$$\Delta\epsilon_0 = -\frac{\gamma^2}{\omega_0} - \frac{\gamma^2}{\pi\omega_0} \sum_{\alpha=L,R} \arctan \frac{\mu_\alpha}{\Gamma_0}. \quad (23)$$

With the same notations, Eq. (A36) gives

$$\begin{aligned} \text{Im}\Sigma_{\text{ho}}^a(\omega) &= \gamma^2\Gamma_0 \left( \frac{[f_L(\omega + \omega_0) + f_R(\omega + \omega_0)]/2}{(\omega + \omega_0)^2 + \Gamma_0^2} \right. \\ &\quad \left. + \frac{1 - [f_L(\omega - \omega_0) + f_R(\omega - \omega_0)]/2}{(\omega - \omega_0)^2 + \Gamma_0^2} \right) \\ &= \frac{\gamma^2\Gamma_0}{2} \sum_{\alpha=L,R} \left( \frac{\Theta(\mu_\alpha - \omega_0 - \omega)}{(\omega + \omega_0)^2 + \Gamma_0^2} + \frac{\Theta(\omega - \mu_\alpha - \omega_0)}{(\omega - \omega_0)^2 + \Gamma_0^2} \right), \end{aligned} \quad (24)$$

which reproduces the result of Ref. 35. Clearly,  $\text{Im}\Sigma_{\text{ho}}^a(\omega) = 0$  unless  $\omega < \mu_L - \omega_0$  and/or  $\omega > \mu_R + \omega_0$ . Since this self-energy is required within an integral for which  $\mu_R \leq \omega \leq \mu_L$  [see Eq. (21)], its contribution to the current appears only when the bias voltage exceeds

$\hbar\omega_0/e$ . Indeed, substituting Eq. (24) in Eq. (21) yields

$$I_{\text{inco}} = \frac{e\gamma^2\Gamma_0^2}{4\pi}\Theta(\mu_L - \mu_R - \hbar\omega_0) \times \left( \int_{\mu_R}^{\mu_L - \omega_0} d\omega \frac{\omega^2 - \Gamma_0^2}{(\omega^2 + \Gamma_0^2)^2} \frac{1}{(\omega + \omega_0)^2 + \Gamma_0^2} + \int_{\mu_R + \omega_0}^{\mu_L} d\omega \frac{\omega^2 - \Gamma_0^2}{(\omega^2 + \Gamma_0^2)^2} \frac{1}{(\omega - \omega_0)^2 + \Gamma_0^2} \right). \quad (25)$$

For  $\omega_0 \gg \Gamma_0$  the integrand in Eq. (25) contains the two Lorentzians shifted from the usual resonance by

$\pm\omega_0$ . The  $\Theta$ -function factor determines how much these Lorentzians contribute to the current. This reinforces the notion that  $I_{\text{inco}}$  is the current due to inelastic processes where a vibration quantum is given to or taken from the oscillator by the transmitted electron. As we discuss below, finite temperatures result in small contributions to the current  $I_{\text{inco}}$  even in the linear-response limit of zero bias voltage.

In a similar way, the real part of the self-energy is found from Eq. (A36)

$$\begin{aligned} \text{Re}\Sigma_{\text{ho}}^a(\omega) &= \gamma^2\Gamma_0 \int \frac{d\omega'}{\pi} \frac{1}{\omega'^2 + \Gamma_0^2} \left( \frac{1 - [f_L(\omega') + f_R(\omega')]/2}{\omega - \omega_0 - \omega'} + \frac{[f_L(\omega') + f_R(\omega')]/2}{\omega + \omega_0 - \omega'} \right) \\ &= \frac{\gamma^2}{2} \left[ \left( \frac{\omega - \omega_0}{(\omega - \omega_0)^2 + \Gamma_0^2} + \frac{\omega + \omega_0}{(\omega + \omega_0)^2 + \Gamma_0^2} \right) + \frac{1}{\pi} \left( \frac{\omega + \omega_0}{(\omega + \omega_0)^2 + \Gamma_0^2} - \frac{\omega - \omega_0}{(\omega - \omega_0)^2 + \Gamma_0^2} \right) \sum_{\alpha=L,R} \arctan \frac{\mu_\alpha}{\Gamma_0} \right. \\ &\quad \left. + \frac{\Gamma_0}{2\pi} \left( \frac{1}{(\omega + \omega_0)^2 + \Gamma_0^2} \sum_{\alpha=L,R} \ln \frac{\mu_\alpha^2 + \Gamma_0^2}{(\omega - \mu_\alpha + \omega_0)^2} - \frac{1}{(\omega - \omega_0)^2 + \Gamma_0^2} \sum_{\alpha=L,R} \ln \frac{\mu_\alpha^2 + \Gamma_0^2}{(\omega - \mu_\alpha - \omega_0)^2} \right) \right], \quad (26) \end{aligned}$$

again reproducing the result of Ref. 35. [A simple interpretation of Eqs. (24) and (26) is given at the end of the Appendix, following Eq. (A36)]. As mentioned, it is convenient to introduce [see Eq. (13)] the total energy shift which depends on the frequency and on the chemical potentials  $\mu_L$  and  $\mu_R$ ,

$$\begin{aligned} \Delta E(\omega, \mu_L, \mu_R) &= \Delta\epsilon_0(\mu_L, \mu_R) + \text{Re}\Sigma_{\text{ho}}^a(\omega, \mu_L, \mu_R) \\ &= \Delta\mu(\omega, \mu_L, \mu_R) + \frac{\gamma^2\Gamma_0}{4\pi} \sum_{\alpha=L,R} \left( \frac{\ln[(\omega - \mu_\alpha - \omega_0)^2/\omega_0^2]}{(\omega - \omega_0)^2 + \Gamma_0^2} - \frac{\ln[(\omega - \mu_\alpha + \omega_0)^2/\omega_0^2]}{(\omega + \omega_0)^2 + \Gamma_0^2} \right), \quad (27) \end{aligned}$$

where

$$\begin{aligned} \Delta\mu(x, \mu_L, \mu_R) &= \frac{\gamma^2}{[(x - \omega_0)^2 + \Gamma_0^2][(x + \omega_0)^2 + \Gamma_0^2]} \left( x(x^2 + \Gamma_0^2 - \omega_0^2) \right. \\ &\quad \left. - \frac{x\omega_0\Gamma_0}{\pi} \sum_{\alpha=L,R} \ln \left[ \frac{\mu_\alpha^2 + \Gamma_0^2}{\omega_0^2} \right] - [(x^2 + \Gamma_0^2)^2 - \omega_0^2(x^2 - \Gamma_0^2)] \frac{1}{\pi\omega_0} \sum_{\alpha=L,R} \arctan \frac{\mu_\alpha}{\Gamma_0} \right). \quad (28) \end{aligned}$$

The factor  $-\gamma^2/\omega_0$ , i.e., the polaron binding energy [see Eq. (23)], is independent of the frequency and of the chemical potentials. Therefore, we may safely absorb it in  $\epsilon_{\text{res}}$  and omit it from Eq. (27). Inspection of Eq. (27) reveals that  $\Delta E$  diverges logarithmically at  $\omega = \mu_\alpha \pm \omega_0$ . This divergence<sup>35</sup> is dictated by the Kramers-Kronig relations once the imaginary part of the self-energy attains a discontinuity [see the discussion following Eq. (24)]. The logarithmic divergence affects the conductance only in the nonlinear regime, and disappears in the linear-response one. However, the density of states is affected by these singularities even in the linear-response regime, see Sec. III. In any case, the logarithmic divergence implies that one should not ignore the frequency dependence of  $\Delta E$  and absorb this energy in  $\epsilon_{\text{res}}$ , as is sometimes done.

### III. THE LINEAR-RESPONSE REGIME

#### A. Zero temperature conductance

In the linear-response regime the bias voltage energy  $eV$  is the smallest energy, and at zero temperature the energy shift and the self-energy are required only at  $\omega = \mu_L = \mu_R \equiv \mu$ , where  $\mu$  is the common Fermi energy of the leads (measured from the resonance energy  $\epsilon_{\text{res}}$ ). Then,  $I_{\text{inco}} = 0$ , and  $I_{\text{co}}$  [Eq. (20)] requires the energy shift  $\Delta E(\mu, \mu, \mu) = \Delta\mu(\mu, \mu, \mu)$  [see Eq. (27)], which is a smooth function of  $\mu$ . Thus, the only contribution to

the conductance from the coupling to the oscillator is

$$\frac{2\pi}{e^2} G_{\text{co}} \Big|_{\text{lin}} = \frac{2\mu\Gamma_0^2}{(\mu^2 + \Gamma_0^2)^2} \Delta E(\mu, \mu, \mu). \quad (29)$$

In the linear-response regime the zeroth-order conductance,  $G_0$ , is

$$\frac{2\pi}{e^2} G_0 \Big|_{\text{lin}} = \frac{\Gamma_0^2}{\mu^2 + \Gamma_0^2}, \quad (30)$$

and we may combine  $G_0$  and  $G_{\text{co}}$  to obtain

$$\frac{2\pi}{e^2} G \Big|_{\text{lin}} = \frac{\Gamma_0^2}{[\mu - \Delta E(\mu, \mu, \mu)]^2 + \Gamma_0^2}. \quad (31)$$

Obviously, this expression is valid up to second-order in the coupling with the oscillator.

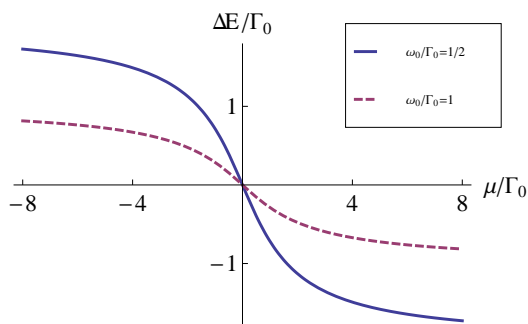


FIG. 1: The function  $\Delta E(\mu, \mu, \mu)$ , Eq. (27), for two representative values of the oscillator frequency,  $\omega_0 = 0.5\Gamma_0$  (solid line), and  $\omega_0 = \Gamma_0$  (dashed line). Here  $\gamma = \Gamma_0$ .

The function  $\Delta E(\mu, \mu, \mu)$  is an odd function of  $\mu$ , and its sign is opposite to that of  $\mu$ , see Fig. 1. Therefore, in the linear-response regime, the effect of the coupling with the oscillator is just to reduce the conductance, *except* at resonance. This can be understood qualitatively as due to the fact that the couplings to the two leads ( $J_0$  in our model) are renormalized downwards, to  $\mathcal{O}(\gamma^2)$ , due to the *same* Franck-Condon-type factor. Therefore, the width of the resonance decreases, but its height, determined by the ratio of the two couplings, is unchanged.<sup>16</sup> The location of the resonance is *not* shifted, since  $\mu - \Delta E(\mu, \mu, \mu) = 0$  only at  $\mu = 0$ , i.e.,  $-\Delta E$  always moves away from the ‘bare’ resonance energy. This behavior is exemplified in Fig. 2, which shows the effect of coupling to the oscillator on the linear-response conductance, for two values of the ‘bare’ width,  $\Gamma_0/\omega_0 = 1/2$  (top) and 4 (bottom).

Clearly, the relative narrowing of the resonance due to the vibrational mode decreases when the ratio  $\Gamma_0/\omega_0$  increases. Quantitatively, the ‘renormalized’ width of the resonance,  $\Gamma$ , is given by the solution of the equation  $\Gamma - \Delta E(\Gamma, \Gamma, \Gamma) = \Gamma_0$ . As can be seen from Fig. 1,  $\Delta E(\mu, \mu, \mu)$  becomes saturated at large  $\mu$ ; the solution for  $\Gamma$  increases towards  $\Gamma_0$  as  $\Gamma_0/\omega_0$  increases. For a qualitative understanding of this effect, we note that at zero

temperature, the oscillator is in the ground state. Then, when the electron moves from, say, the left lead to the virtual state on the dot, the term  $\gamma(b + b^\dagger)c_0^\dagger c_0$  in the dot Hamiltonian, Eq. (4), shifts the center of the oscillator motion by the order of  $\gamma/\omega_0$  (in units of the oscillator’s zero-point displacement). However, this shift is fully realized only when the dwell-time of the electron on the dot,  $\Gamma_0^{-1}$ , is longer than the response-time of the oscillator, governed by  $\omega_0$ , i.e.  $\Gamma_0/\omega_0 \ll 1$ . In this limit, the coupling matrix element  $J_0$  will be reduced by the overlap integral between the shifted and the un-shifted oscillator wave functions, which is of order  $\exp[-(\gamma/\omega_0)^2/2]$ , resulting in a relative narrowing of the resonance.<sup>19</sup>

Indeed, at small  $\gamma/\omega_0$  (so that the perturbative expansion is valid) and for small  $\Gamma_0/\omega_0$  we find that  $\Gamma/\Gamma_0$  approaches the Franck-Condon factor  $\exp[-(\gamma/\omega_0)^2]$  (which becomes  $1 - (\gamma/\omega_0)^2$  in our order  $\gamma^2$  approximation). This can be seen directly from Eqs. (26): when  $\omega_0 \gg \{|\mu|, \Gamma_0\}$ ,  $\text{Re}\Sigma_{\text{ho}}^a(\omega)$  is dominated by the first term in the large brackets on the second line, which is independent of the Fermi functions. Therefore, in this limit  $\Delta E(\mu, \mu, \mu)$  does not depend on the many-body effects contained in these Fermi functions, and the simple single particle Franck-Condon result is reproduced. Indeed, in this limit one has  $\Delta E(\mu, \mu, \mu) = \Delta\mu(\mu, \mu, \mu) \approx -\mu\gamma^2/\omega_0^2 + \mathcal{O}(\mu\Gamma_0\gamma^2/\omega_0^3)$ , and therefore  $\Gamma \approx \Gamma_0(1 - \gamma^2/\omega_0^2)$ . In contrast, when  $\Gamma_0 \gg \omega_0$  (bottom panel of Fig. 2) the electron leaves the dot before the oscillator has responded to its presence, and the Franck-Condon blockade effect is much weakened. In our calculation, part of this blocking involves the Fermi functions on the leads [all the terms except the first in Eq. (26)]. This dependence on the chemical potentials in the leads reflects the many-body effects on the leads, which seem to weaken the Franck-Condon blockade. So far, we have discussed the Franck-Condon narrowing only for zero temperature and zero bias voltage. However, the modified narrower shape of the resonances will also affect integrals over energy, causing apparently similar effects at finite temperatures and at a finite bias voltage.

Another remarkable aspect is that at zero temperature the linear-response conductance exhibits no side-bands as a function of the gate voltage (modeled here by the common  $\mu$  measured from  $\epsilon_{\text{res}}$ ), when  $\mu$  crosses the oscillator frequency. This has been emphasized in Ref. 16, contrary to certain findings in the literature (see for example Refs. 22 and 25). Finite temperatures may generate small satellites, as discussed in Sec. III C. The absence of the side-bands in the linear-response conductance at the oscillator frequency, as the gate voltage is swept, may appear at first sight somewhat surprising. However, it is their appearance at zero bias voltage and zero temperature which is in fact un-physical. A structure in the linear-response conductance at  $\mu = \pm\omega_0$  will mean that after passing, the electron leaves the dot in an excited state, even at zero temperature. As the electron begins and ends at almost the same energy, energy conservation does not allow it to excite the oscillator.

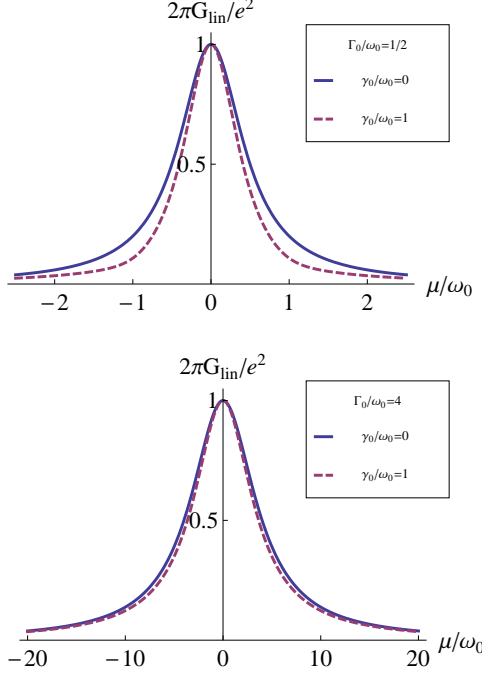


FIG. 2: The dimensionless linear-response conductance, Eq. (31), for two representative values of the ratio  $\Gamma_0/\omega_0$ , 0.5 (top panel) and 4 (bottom panel). It can be seen that the conductance (dashed line) is *always* smaller than that obtained in the absence of the coupling with the oscillator (depicted by the solid line).<sup>42</sup>

### B. The zero-temperature density of states

The situation is very different when one looks at the local single-particle density of states on the dot,  $N(\omega)$ , given by

$$N(\omega) = -\frac{1}{\pi} \text{Im}G_{00}(\omega). \quad (32)$$

This density of states is accessible, in principle, via local STM  $I - V$  measurements. We note that  $N(\omega)$  is the nontrivial part of the integrand in the basic Eq. (9) for the current. Here we actually calculate it only at equilibrium, which is appropriate for the linear transport regime. For  $\mu_L = \mu_R = \mu$ , this quantity becomes

$$N(\omega) = \frac{1}{\pi} \frac{\Gamma_0 + \text{Im}\Sigma_{\text{ho}}^a(\omega)}{[\omega - \Delta E(\omega, \mu, \mu)]^2 + [\Gamma_0 + \text{Im}\Sigma_{\text{ho}}^a(\omega)]^2}, \quad (33)$$

where  $\text{Im}\Sigma_{\text{ho}}^a(\omega)$  is given by Eq. (24), and  $\Delta E(\omega, \mu, \mu)$  is given by Eqs. (26), (27), and (28). Inspection of those expressions reveals that when  $\mu = 0$ , i.e., the common chemical potential of the leads is aligned with the resonance level on the dot, the density of states Eq. (33) is even in the frequency, while at off resonance (where  $\mu \neq 0$  in our notations) it is not. In the first case, there will be equal weights for a hole (an electron) excitation

corresponding to an excited oscillator and an electron (a hole). In the second, those weights are not equal. In particular, when  $\mu > 0$ , i.e., the common chemical potential of the leads is above the level on the dot, and there is more weight to the hole formation.

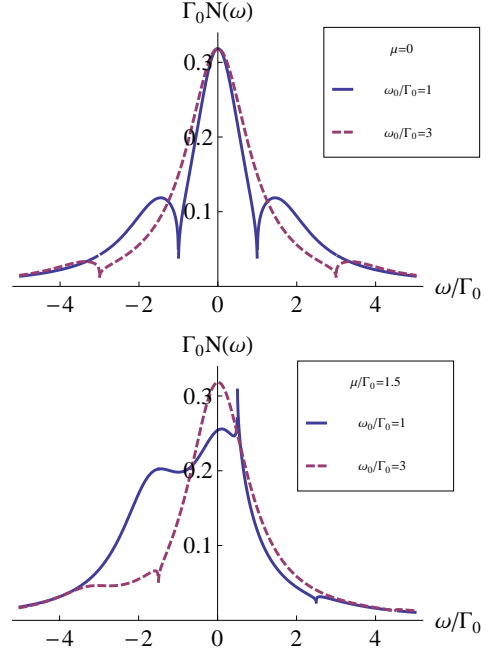


FIG. 3: The local density of states on the dot, Eq. (33), as a function of the energy  $\omega$  for  $\mu = 0$  (top panel) and for  $\mu = 1.5\Gamma_0$  (bottom panel). The solid lines correspond to  $\omega_0 = \Gamma_0$ , while  $\omega_0 = 3\Gamma_0$  for the dashed lines (here,  $\gamma = \Gamma_0$ ). All the graphs should go to zero at  $\omega = \pm\omega_0$ .

The local density of states  $N(\omega)$  is plotted in Fig. 3 at resonance,  $\mu = 0$  (upper panel), and off-resonance,  $\mu = 1.5\Gamma_0$  (lower panel). Both figures show structures around  $\omega = \mu \pm \omega_0$ , which become smaller as  $\omega_0$  increases. Each of these structures contains two ingredients: first,  $\Delta E$  diverges logarithmically near  $\omega = \mu \pm \omega_0$ , resulting in the vanishing of  $N(\omega)$  at these frequencies. Since these singularities are very narrow, the plots miss showing the actual vanishing of  $N(\omega)$  at these points. The situation is somewhat more complicated for  $\mu > 0$  and  $\omega = \mu - \omega_0$  (corresponding to the vicinity of  $\omega_0/\Gamma_0 = 0.5$  for the full line in the lower panel of Fig. 3). In that case, the energy difference  $\omega - \Delta E(\omega, \mu, \mu)$  changes sign as one approaches the singular point, and therefore  $N(\omega)$  first increases and only then decreases quickly to zero at  $\omega = \mu - \omega_0$ . The plot picks up the initial increase, and misses the very narrow dip.

The second effect arises from  $\text{Im}\Sigma_{\text{ho}}^a(\omega)$ , which modifies the width of the original resonance and creates the inelastic resonances. As can be seen from Eq. (24), this term contains contributions from two ‘resonances’, at  $\omega = \pm\omega_0$ . However, the left (right) hand side resonance is included only for  $\omega < \mu - \omega_0$  ( $\omega > \mu + \omega_0$ ). For  $|\mu| < \omega_0$ , this causes a discontinuous increase in  $N(\omega)$

for  $\omega$  below (above)  $\mu - \omega_0$  ( $\mu + \omega_0$ ). The deep dips at  $\omega = \mu \pm \omega_0$  and the increased density of states beyond these energies create peaks in  $N(\omega)$  at  $\omega > \mu + \omega_0$  and at  $\omega < \mu - \omega_0$ , which can be identified as the side-bands (see top panel in Fig. 3). For  $\mu > \omega_0$ , the behavior for  $\omega \lesssim \mu - \omega_0$  is more complex, but the general features remain the same (lower panel in the figure). Note that our calculation shows only two such ‘‘side-bands’’, since we work to second order in the coupling with the oscillator. Note also that the side-bands would not be as clear had we absorbed  $\Delta E$  as a ‘constant’ in  $\epsilon_{\text{res}}$ .

### C. Finite temperatures

At finite temperatures, the linear-response conductance is given by [see Eq. (9)]

$$\frac{2\pi}{e^2} G|_{\text{lin}} = \Gamma_0 \int d\omega \left( \beta \frac{e^{\beta(\omega-\mu)}}{(e^{\beta(\omega-\mu)} + 1)^2} \right) \text{Im} G_{00}^a(\omega). \quad (34)$$

Using the expansion of Eq. (13), and the expressions in Eq. (A36), and substituting  $\mu_L = \mu_R = \mu$  for linear-response, yields

$$\Delta E(\omega) = \gamma^2 \int \frac{d\omega'}{\pi} \frac{\Gamma_0}{\omega'^2 + \Gamma_0^2} \frac{\omega - \omega'}{(\omega - \omega')^2 - \omega_0^2} \times \left( \coth \frac{\beta\omega_0}{2} + \frac{\omega - \omega'}{\omega_0} \tanh \frac{\beta(\omega' - \mu)}{2} \right), \quad (35)$$

and

$$\text{Im} \Sigma_{\text{ho}}^a(\omega) = \frac{\gamma^2}{2} \sum_{s=\pm} \frac{\Gamma_0}{(\omega - s\omega_0)^2 + \Gamma_0^2} \times \left( \coth \frac{\beta\omega_0}{2} + s \tanh \frac{\beta(\omega - s\omega_0 - \mu)}{2} \right). \quad (36)$$

Figure 4 portrays the contribution of  $I_{\text{inco}}$ , Eq. (18), to the linear-response conductance. We plot only this contribution, which arises from the inelastic processes, in order to exhibit the channel-opening due to the finite temperature. The contribution of  $I_{\text{co}}$  is smooth, so it does not have drastic effects at finite temperature. Scaling  $I_{\text{inco}}$  by  $\beta\Gamma_0 \exp[-\beta\omega_0]$ , it is seen that the curves plotted for various temperatures approach an asymptotic limiting form for large  $\beta\Gamma_0$ , exhibiting a reduction of the conductance near  $\mu = 0$  and peaks slightly above (below)  $\mu = \omega_0$  ( $\mu = -\omega_0$ ). This structure could have been described as having side-bands; however, the peaks decay exponentially (as  $\exp[-\beta\omega_0]$ ) at low temperatures. This factor arises directly from the low temperature behavior of the large brackets in Eq. (36), and is also understandable intuitively: the side-bands can contribute only if excitations by the oscillator energy  $\hbar\omega_0$  are allowed. Those appear with the Boltzmann factor  $\exp[-\beta\omega_0]$ . As the temperature increases, the structure portrayed in Fig. 4 broadens and gradually becomes smeared.

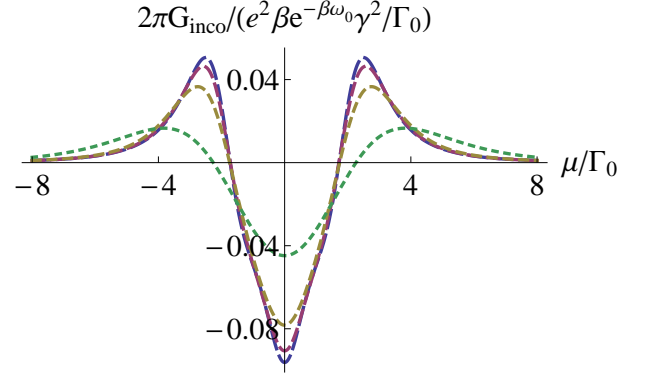


FIG. 4: The linear-response conductance resulting from  $I_{\text{inco}}$ , for  $\beta\Gamma_0 = 1, 3, 6$  and  $12$  (increasing dash sizes). Here  $\omega_0 = 2\Gamma_0$ , and all energies are in units of  $\Gamma_0$ .

### IV. THE ZERO TEMPERATURE DIFFERENTIAL CONDUCTANCE

The differential conductance is the derivative of the current with respect to the bias voltage,  $V = (\mu_L - \mu_R)/e$  [however, for finite bias voltage, note the discussion following Eq. (9)]. Differentiating Eq. (19) with respect to  $V$ , the zeroth-order conductance is

$$\frac{2\pi}{e^2} G_0 = \frac{1}{2} \left( \frac{\Gamma_0^2}{\mu_L^2 + \Gamma_0^2} + \frac{\Gamma_0^2}{\mu_R^2 + \Gamma_0^2} \right). \quad (37)$$

Similarly, differentiating Eq. (20) gives

$$\frac{2\pi}{e^2} G_{\text{co}} = \frac{2\pi}{e^2} G_{\text{co}}^{(1)} + \frac{2\pi}{e^2} G_{\text{co}}^{(2)}, \quad (38)$$

where

$$\frac{2\pi}{e^2} G_{\text{co}}^{(1)} = \sum_{\alpha=L,R} \frac{\Gamma_0^2 \mu_\alpha}{(\mu_\alpha^2 + \Gamma_0^2)^2} \Delta E(\omega = \mu_\alpha, \mu_L, \mu_R), \quad (39)$$

and

$$\frac{2\pi}{e^2} G_{\text{co}}^{(2)} = 2\Gamma_0^2 \int_{\mu_R}^{\mu_L} d\omega \frac{\omega}{(\omega^2 + \Gamma_0^2)^2} \frac{d\Delta E(\omega)}{d(\mu_L - \mu_R)}. \quad (40)$$

Using Eq. (27), we have

$$\frac{d\Delta E(\omega)}{d(\mu_L - \mu_R)} = \frac{\gamma^2 \Gamma_0}{2\pi} \left( \frac{1}{\mu_R^2 + \Gamma_0^2} \frac{(\omega - \mu_R)^2 / \omega_0}{(\omega - \mu_R)^2 - \omega_0^2} - \frac{1}{\mu_L^2 + \Gamma_0^2} \frac{(\omega - \mu_L)^2 / \omega_0}{(\omega - \mu_L)^2 - \omega_0^2} \right). \quad (41)$$

A rather lengthy computation yields



$$\begin{aligned}
\frac{2\pi}{e^2} G_{\text{co}} = & \sum_{\alpha=L,R} \frac{\mu_\alpha \Gamma_0^2 \Delta\mu(\mu_\alpha, \mu_L, \mu_R)}{(\mu_\alpha^2 + \Gamma_0^2)^2} + \frac{\gamma^2 \Gamma_0^3}{2\pi\omega_0} \left[ \frac{\mu_L^2 - \mu_R^2}{(\mu_L^2 + \Gamma_0^2)(\mu_R^2 + \Gamma_0^2)} \right]^2 \\
& + \frac{\gamma^2 \Gamma_0^3}{4\pi} \sum_{\alpha=L,R} \left( \frac{F(\mu_\alpha, \mu_\alpha - \omega_0) - F(\mu_\alpha, \mu_\alpha + \omega_0)}{\mu_\alpha^2 + \Gamma_0^2} + \frac{F(\mu_\alpha, \mu_{\bar{\alpha}} + \omega_0) - F(\mu_{\bar{\alpha}}, \mu_\alpha - \omega_0)}{\mu_{\bar{\alpha}}^2 + \Gamma_0^2} \right) \\
& + \frac{\Gamma_0^3 \gamma^2 \omega_0}{4\pi} \ln \left[ \frac{(\mu_L - \mu_R + \omega_0)^2}{\omega_0^2} \right] \left( \frac{\Gamma_0^2 - \mu_L(\mu_L + \omega_0)}{(\mu_L^2 + \Gamma_0^2)^2 ((\mu_L + \omega_0)^2 + \Gamma_0^2)^2} + \frac{\Gamma_0^2 - \mu_R(\mu_R - \omega_0)}{(\mu_R^2 + \Gamma_0^2)^2 ((\mu_R - \omega_0)^2 + \Gamma_0^2)^2} \right) \\
& + \frac{\Gamma_0^3 \gamma^2 \omega_0}{4\pi} \ln \left[ \frac{(\mu_L - \mu_R - \omega_0)^2}{\omega_0^2} \right] \left( \frac{\Gamma_0^2 - \mu_L(\mu_L - \omega_0)}{(\mu_L^2 + \Gamma_0^2)^2 ((\mu_L - \omega_0)^2 + \Gamma_0^2)^2} + \frac{\Gamma_0^2 - \mu_R(\mu_R + \omega_0)}{(\mu_R^2 + \Gamma_0^2)^2 ((\mu_R + \omega_0)^2 + \Gamma_0^2)^2} \right), \quad (42)
\end{aligned}$$

where  $\Delta\mu$  is given by Eq. (28), and we have defined

$$\begin{aligned}
F(x, y) = & \frac{1}{(y^2 + \Gamma_0^2)^2} \left( \frac{(x+y)(y^2 + \Gamma_0^2)}{x^2 + \Gamma_0^2} \right. \\
& \left. - y \ln \left[ \frac{x^2 + \Gamma_0^2}{\omega_0^2} \right] + \frac{\Gamma_0^2 - y^2}{\Gamma_0} \arctan \frac{x}{\Gamma_0} \right). \quad (43)
\end{aligned}$$

Also,  $\bar{\alpha}$  marks the lead which is not  $\alpha$ . One observes that when  $\mu_L = \mu_R$ , then  $G_{\text{co}}$  is fully given by only the first sum in Eq. (42), reducing to the linear-response result (29).

Finally, the differential conductance resulting from the current  $I_{\text{inco}}$ , Eq. (25), is

$$\begin{aligned}
\frac{2\pi}{e^2} G_{\text{inco}} = & \frac{\gamma^2 \Gamma_0^2}{2} \Theta(\mu_L - \mu_R - \omega_0) \\
& \times \left( \frac{\mu_L^2 (\mu_L - \omega_0)^2 - \Gamma_0^4}{(\mu_L^2 + \Gamma_0^2)^2 ((\mu_L - \omega_0)^2 + \Gamma_0^2)^2} \right. \\
& \left. + \frac{\mu_R^2 (\mu_R + \omega_0)^2 - \Gamma_0^4}{(\mu_R^2 + \Gamma_0^2)^2 ((\mu_R + \omega_0)^2 + \Gamma_0^2)^2} \right). \quad (44)
\end{aligned}$$

At the threshold bias voltage,  $eV = \mu_L - \mu_R = \omega_0$ , this contribution jumps from zero to

$$\frac{2\pi}{e^2} \Delta G_{\text{inco}} = \gamma^2 \Gamma_0^2 \frac{\mu_L^2 \mu_R^2 - \Gamma_0^4}{(\mu_L^2 + \Gamma_0^2)^2 (\mu_R^2 + \Gamma_0^2)^2}. \quad (45)$$

Since at  $eV = \omega_0$  the chemical potentials are  $\mu_L = \mu + \omega_0/2$  and  $\mu_R = \mu - \omega_0/2$ , it follows that the conductance jumps *downwards* when the common chemical potential of the leads (measured from the resonance level) is in the range

$$\max[0, (\omega_0/2)^2 - \Gamma_0^2] \leq \mu^2 \leq (\omega_0/2)^2 + \Gamma_0^2. \quad (46)$$

Note that the range in which the conductance jumps downwards is shrinking as  $\omega_0/\Gamma_0$  becomes larger. Since the “bare” elastic transparency of the junction is given by  $\mathcal{T} = \Gamma_0^2/(\mu^2 + \Gamma_0^2)$ , the condition (46) can be put in the form

$$\frac{1}{2 + (\omega_0/2\Gamma_0)^2} \equiv \mathcal{T}_1 \leq \mathcal{T} \leq \mathcal{T}_2 \equiv \min[1, (2\Gamma_0/\omega_0)^2]. \quad (47)$$

One notes that the lower border-line transparency<sup>33,34</sup>  $\mathcal{T}_1$  reaches the “universal” value 1/2 (with  $\mathcal{T}_2 = 1$ ) only<sup>35</sup> in the limit of a very broad resonance,  $\Gamma_0 \gg \omega_0$ , where the effects of the vibrational excitations are smeared within the original resonance. As the ratio  $\omega_0/\Gamma_0$  increases, both  $\mathcal{T}_1$  and  $\mathcal{T}_2$  decrease and approach each other, so that the region with a negative step in  $G_{\text{inco}}$  narrows down in this physically relevant region.

For  $V > 0$ , the logarithmic divergence in  $G_{\text{co}}$  arises only due to the last term in Eq. (42). Near  $eV = \hbar\omega_0$ , the coefficient of this term contains the factor  $\Gamma_0^2 - \mu_L \mu_R = \Gamma_0^2 + (\omega_0/2)^2 - \mu^2$ , which is positive for all  $\mathcal{T} > \mathcal{T}_1$ . Since the argument of the log is small near  $eV = \hbar\omega_0$ , this implies a negative divergence of this term in this range (and a positive one for  $\mathcal{T} < \mathcal{T}_1$ ). Interestingly, the logarithmic term does not change sign at  $\mathcal{T}_2$ , although the step in  $G_{\text{inco}}$  does change sign there. We note that the Kramers-Kronig relation, relating these two singularities, applies only to the real and imaginary parts of the self-energy, and not to the corresponding contributions to the differential conductance.

Figure 5 shows the total conductance  $G = G_0 + G_{\text{co}} + G_{\text{inco}}$ , as well as the two separate contributions from the coupling to the oscillator  $G_{\text{co}}$  and  $G_{\text{inco}}$ , for  $\omega_0 = 3\Gamma_0$  and for five values of  $\mathcal{T}$ . The plot for  $G_{\text{co}}$  does not contain the first term in Eq. (42), which was incorporated into Eq. (37) by the replacements  $\mu_\alpha \rightarrow \mu_\alpha - \Delta\mu(\mu_\alpha, \mu_L, \mu_R)$ . Clearly, there are no visible singularities when  $\mathcal{T} = \mathcal{T}_1$ , where the coefficients of both the logarithmic term and the discontinuity vanish (there remain effects for higher derivatives of the current). The former singularity survives at  $\mathcal{T} = \mathcal{T}_2$ , where the discontinuity vanishes (although more steeply than near  $\mathcal{T}_1$ ). The logarithmic divergence is indeed positive for  $\mathcal{T} < \mathcal{T}_1$ . Also, the magnitudes of both the jump and the logarithmic divergence are large at large bare transparencies  $\mathcal{T}$ , and decrease with decreasing  $\mathcal{T}$ . It should be kept in mind that the apparent divergence in  $G_{\text{co}}$  results from our expansion in powers of  $\gamma$ , which breaks down very close to the threshold  $V = \hbar\omega_0/e$ .

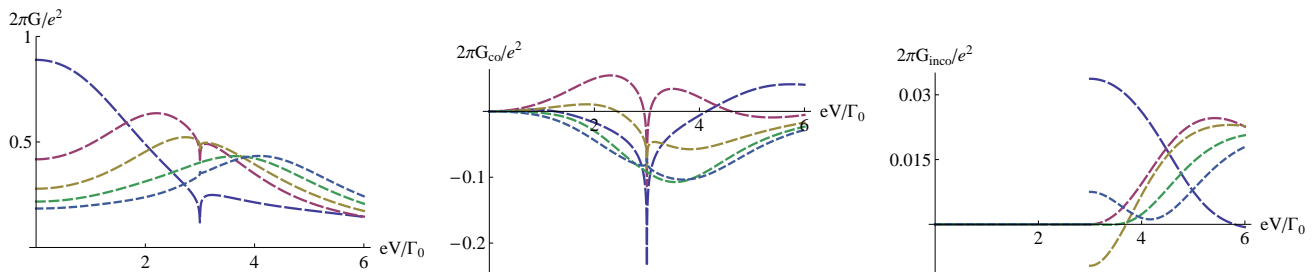


FIG. 5: The total differential conductance (left panel) and the contributions to the conductance from the coupling to the vibrational mode,  $G_{\text{co}}$  (middle panel, containing the logarithmic divergence) and  $G_{\text{inco}}$  (right panel, containing the discontinuity;  $G_{\text{inco}} = 0$  for  $eV < \hbar\omega_0$ , and the jumps in the various conductances at the thresholds are seen as the lapses in the curves) as function of the bias voltage, for  $\omega_0 = 3\Gamma_0$ , and five different values of the zeroth-order transmission  $\mathcal{T} = 0.2$ ,  $\mathcal{T}_1 = 4/17$ ,  $0.3$ ,  $\mathcal{T}_2 = 4/9$ ,  $0.9$  (dash sizes increase with  $\mathcal{T}$ , appearing in increasing order at small  $V$  in the left panel). Here  $\gamma = \Gamma_0$ .

## V. SUMMARY

Although several of our formal results have already been obtained by Mitra *et al.*<sup>16</sup> and by Egger and Gogolin,<sup>35</sup> our paper has used these results for a critical discussion of several physically relevant issues which have been debated in the literature. Specifically, we have obtained and highlighted the following points:

(A) At zero temperature, the resonance peak in the linear-response conductance always narrows down due to the coupling to the vibrational mode. However, this narrowing down is given by the Franck-Condon factor only for narrow resonances, and when one may ignore the Fermi statistics of the electrons on the leads. When  $\Gamma_0 \gg \omega_0$ , the electron dwell-time on the dot is short and therefore the relative narrowing is much smaller.

(B) Contrary to claims in the literature, the linear-response conductance does not exhibit any side-bands at zero temperature. Small satellites, of order  $\exp[-\beta\omega_0]$ , do arise at finite temperatures, where the excitation of the vibrational mode becomes possible.

(C) The coupling to the vibrational modes does show up in the single-particle density of states, which exhibits two singularities at the frequencies  $\omega = \mu \pm \omega_0$  which correspond to the opening of the inelastic channel in which the vibrational mode remains excited. (We find only two singular points, because we expand the results only up to second order in the coupling to the vibrational mode.) These include discontinuities, due to the imaginary part of the self-energy, and logarithmic singularities, due to the real part of the self-energy. The latter result in deep dips in the density of states around each threshold, creating apparent side-bands at frequencies which exceed these thresholds. Although a logarithmic singularity implies the inapplicability of the perturbative expansion very close to the inelastic thresholds, the predictions of dips and satellites in the density of states can probably be trusted out of these narrow regions.

(D) The same singularities also generate discontinuities and logarithmic divergences in the differential conduc-

tance at and around the thresholds  $eV = \pm\hbar\omega_0$ . The signs of the discontinuities are usually positive, but they become *negative* within a finite range of the bare elastic transparency of the junction, shrinking progressively as  $\omega_0/\Gamma_0$  is increased. The “universal ratio”<sup>33,34</sup> is obtained only<sup>35</sup> in the limit  $\omega_0/\Gamma_0 \ll 1$ , in which the state with an electron on the dot and the vibrational mode excited is not well-defined. In contrast, the logarithmic divergences remain negative for a rather broad range of bare transparencies, indicating the breakdown of our perturbative expansion very close to the inelastic thresholds.

(E) Contrary to some claims in the literature, our results are quite different from those based on the single-electron transmission, which ignore the Fermi seas in the leads.

It would be useful to test some of these predictions in experiments or in other theoretical calculations.

## Acknowledgments

This work was initiated by many illuminating discussions with Doron Cohen. It was supported by the German Federal Ministry of Education and Research (BMBF) within the framework of the German-Israeli project cooperation (DIP), by the US-Israel Binational Science Foundation (BSF), by the Israel Science Foundation (ISF) and by the Converging Technologies Program of the Israel Science Foundation (ISF).

## APPENDIX A: THE KELDYSH GREEN FUNCTIONS

We obtain the Green functions of our system by solving the Dyson equations up to second order in the coupling  $\gamma$ . In this procedure, we use the following relation<sup>43</sup> for the lesser product of two Green functions,

$$(AB)^< = A^r B^< + A^< B^a, \quad (\text{A1})$$

and similarly for the greater product of two Green functions, denoted by the superscript  $>$ . Here,

$$\begin{aligned} G_{ab}^<(\omega) &= i \int dt e^{i\omega t} \langle b^\dagger a(t) \rangle, \\ G_{ab}^>(\omega) &= -i \int dt e^{i\omega t} \langle a(t) b^\dagger \rangle. \end{aligned} \quad (\text{A2})$$

Note that when the operators  $a$  and  $b$  are identical,  $G^<$  and  $G^>$  are purely imaginary. Another property of these Green functions (for general  $a$  and  $b$ ) is

$$G^<(\omega) - G^>(\omega) = G^a(\omega) - G^r(\omega), \quad (\text{A3})$$

where  $G^r$  ( $G^a$ ) is the retarded (advanced) Green function,

$$\begin{aligned} G_{ab}^r(\omega) &= -i \int_0^\infty dt e^{i(\omega+i0^+)t} \langle [a(t), b^\dagger]_+ \rangle, \\ G_{ab}^a(\omega) &= i \int_{-\infty}^0 dt e^{i(\omega-i0^+)t} \langle [a(t), b^\dagger]_+ \rangle. \end{aligned} \quad (\text{A4})$$

For brevity, the frequency  $\omega$  does not appear explicitly in most of the equations below.

The Dyson equation of the Green function on the dot,  $G_{00}$ , reads

$$G_{00} = g_0 \left( 1 + \sum_k V_k G_{k0} + \sum_p V_p G_{p0} + \gamma G_{0Q0} \right). \quad (\text{A5})$$

Here,  $g_0$  is the free Green function of the dot (in the absence of the coupling with the harmonic oscillator and with the leads), i.e.,  $g_0 = (\omega - \epsilon_0)^{-1}$ . The other Green functions in Eq. (A5) are those mixing the leads and the dot operators,

$$G_{k(p)0} = \lll c_{k(p)}; c_0^\dagger \ggg, \quad (\text{A6})$$

and the one mixing the dot and the oscillator operators,

$$G_{0Q0} = \lll c_0(b + b^\dagger); c_0^\dagger \ggg. \quad (\text{A7})$$

In the notations  $\lll; \ggg$ , the first (second) operator (or a product of operators) is the operator denoted by  $a$  ( $b$ ) in Eqs. (A2) and (A4).

The Dyson equations of the Green functions (A6) are

$$G_{k(p)0} = g_{k(p)} V_{k(p)} G_{00}. \quad (\text{A8})$$

Here  $g_{k(p)}$  is the free Green function of the left (right) lead,

$$\begin{aligned} g_{k(p)}^r &= \frac{1}{\omega - \epsilon_{k(p)} + i0^+} = \left( g_{k(p)}^a \right)^*, \\ g_{k(p)}^< &= (g_{k(p)}^a - g_{k(p)}^r) f_{L(R)}(\omega) \\ &= 2\pi i \delta(\epsilon_{k(p)} - \omega) f_{L(R)}(\omega), \end{aligned} \quad (\text{A9})$$

where  $f_{L(R)}$  is the Fermi distribution of the left (right) reservoir. As mentioned above, we assume that the two

leads are identical except for their different Fermi functions. It therefore follows that

$$\sum_k V_k G_{k0} + \sum_p V_p G_{p0} = \Sigma_0 G_{00}, \quad (\text{A10})$$

where  $\Sigma_0$  is the self-energy due to the coupling of the dot with the leads,

$$\begin{aligned} \Sigma_0^r &= \sum_k \frac{V_k^2}{\omega - \epsilon_k + i0^+} + \sum_p \frac{V_p^2}{\omega - \epsilon_p + i0^+} \\ &\equiv 2 \sum_k \frac{V_k^2}{\omega - \epsilon_k + i0^+}, \end{aligned} \quad (\text{A11})$$

and

$$\Sigma_0^< = \frac{\Sigma_0^a - \Sigma_0^r}{2} (f_R + f_L). \quad (\text{A12})$$

Thus, the Dyson equation (A5) of the dot Green function becomes

$$\left( g_0^{-1} - \Sigma_0^r \right) G_{00}^r = 1 + \gamma G_{0Q0}^r, \quad (\text{A13})$$

and

$$\left( g_0^{-1} - \Sigma_0^r \right) G_{00}^< = \Sigma_0^< G_{00}^a + \gamma G_{0Q0}^<. \quad (\text{A14})$$

In particular, the dot Green functions in the absence of the coupling with the harmonic oscillator,  $\mathcal{G}_{00}$ , are

$$\begin{aligned} \mathcal{G}_{00}^r &= \left( \omega - \epsilon_0 - \Sigma_0^r \right)^{-1}, \\ \mathcal{G}_{00}^< &= \mathcal{G}_{00}^r \Sigma_0^< \mathcal{G}_{00}^a = \frac{f_L + f_R}{2} (\mathcal{G}_{00}^a - \mathcal{G}_{00}^r). \end{aligned} \quad (\text{A15})$$

The self-energy coming from the coupling with the harmonic oscillator results from the Green function  $G_{0Q0}$ , Eq. (A5). Its Dyson equation reads

$$\begin{aligned} G_{0Q0} &= \left( \langle b + b^\dagger \rangle \right. \\ &\quad \left. + \sum_k V_k G_{0Qk} + \sum_p V_p G_{0Qp} + \gamma G_{0Q0Q} \right) g_0, \end{aligned} \quad (\text{A16})$$

where

$$G_{0Qk(p)} = \lll c_0(b + b^\dagger); c_{k(p)}^\dagger \ggg, \quad (\text{A17})$$

and

$$G_{0Q0Q} = \lll c_0(b + b^\dagger); (b + b^\dagger) c_0^\dagger \ggg. \quad (\text{A18})$$

It is straightforward to obtain

$$\sum_k V_k G_{0Qk}^r + \sum_p V_p G_{0Qp}^r = \Sigma_0^r G_{0Q0}^r, \quad (\text{A19})$$

and

$$\sum_k V_k G_{0Qk}^< + \sum_p V_p G_{0Qp}^< = \Sigma_0^a G_{0Q0}^< + \Sigma_0^< G_{0Q0}^r. \quad (\text{A20})$$

Thus we find from Eq. (A16) that

$$(g_0^{-1} - \Sigma_0^r) G_{0Q0}^r = \langle b + b^\dagger \rangle + \gamma G_{0Q0Q}^r, \quad (\text{A21})$$

and

$$(g_0^{-1} - \Sigma_0^a) G_{0Q0}^< = \Sigma_0^< G_{0Q0}^r + \gamma G_{0Q0Q}^<. \quad (\text{A22})$$

Inserting the result (A21) into Eq. (A13) gives that the retarded Green function on the dot, up to second order in the coupling  $\gamma$ , is

$$G_{00}^r = \left( \omega - \epsilon_0 - \gamma \langle b + b^\dagger \rangle - \Sigma_0^r - \Sigma_{\text{ho}}^r \right)^{-1}, \quad (\text{A23})$$

where we have defined

$$\Sigma_{\text{ho}}^r = \gamma^2 G_{0Q0Q}^r. \quad (\text{A24})$$

An analogous result holds for the advanced Green function. Using this result and Eq. (A22) in Eq. (A14) yields the Keldysh Green function on the dot (again, up to second order in  $\gamma$ ),

$$G_{00}^< = G_{00}^r \left( \Sigma_0^< + \Sigma_{\text{ho}}^< \right) G_{00}^a, \quad (\text{A25})$$

with

$$\Sigma_{\text{ho}}^< = \gamma^2 G_{0Q0Q}^<. \quad (\text{A26})$$

It is hence found that the coupling with the harmonic oscillator modifies the dot Green function in two ways.

Firstly, it adds the term  $\Sigma_{\text{ho}} = \gamma^2 G_{0Q0Q}$  to the self-energy. This contribution is calculated below. Secondly, it shifts the resonance level by the amount

$$\Delta\epsilon_0 = \gamma \langle b + b^\dagger \rangle = -\frac{2\gamma^2}{\omega_0} \langle c_0^\dagger c_0 \rangle = \frac{2i\gamma^2}{\omega_0} \int \frac{d\omega}{2\pi} \mathcal{G}_{00}^<(\omega). \quad (\text{A27})$$

This result is found by employing perturbation theory. To first order, the oscillator wave functions can be written in the form

$$\Psi_{n'} = |n'\rangle + \gamma c_0^\dagger c_0 \sum_{n \neq n'} \frac{\langle n|b + b^\dagger|n'\rangle}{\omega_0(n' - n)} |n\rangle, \quad (\text{A28})$$

and consequently the diagonal ( $n'n'$ ) matrix element of  $b + b^\dagger$  is

$$\begin{aligned} \frac{2\gamma}{\omega_0} c_0^\dagger c_0 \sum_{n \neq n'} \frac{\langle n|b|n'\rangle \langle n'|b^\dagger|n\rangle + \langle n|b^\dagger|n'\rangle \langle n'|b|n\rangle}{n' - n} \\ = -\frac{2\gamma}{\omega_0} c_0^\dagger c_0. \end{aligned} \quad (\text{A29})$$

The average of  $c_0^\dagger c_0$  is needed to zeroth order in the coupling with the oscillator, and therefore is expressed in terms of the Green function (A15), leading to Eq. (A27).

It remains to compute the Green function  $G_{0Q0Q}$ , Eq. (A18). As we work up to second order in the coupling  $\gamma$ , it is enough to find this function in the absence of the coupling to the oscillator. At this order, the electron operators and the oscillator operators are decoupled. For example, using the definitions of the Keldysh Green functions, Eqs. (A2) and (A4),

$$\begin{aligned} G_{0Q0Q}^r(\omega) &= -i \int_0^\infty dt e^{i\omega t} \left( \langle (b(t) + b^\dagger(t))(b + b^\dagger) \rangle \langle c_0(t) c_0^\dagger \rangle + \langle (b + b^\dagger)(b(t) + b^\dagger(t)) \rangle \langle c_0^\dagger c_0(t) \rangle \right) \\ &= \langle bb^\dagger \rangle \int_0^\infty e^{i(\omega - \omega_0)t} \mathcal{G}_{00}^>(t) + \langle b^\dagger b \rangle \int_0^\infty e^{i(\omega + \omega_0)t} \mathcal{G}_{00}^>(t) - \langle bb^\dagger \rangle \int_0^\infty e^{i(\omega + \omega_0)t} \mathcal{G}_{00}^<(t) - \langle b^\dagger b \rangle \int_0^\infty e^{i(\omega - \omega_0)t} \mathcal{G}_{00}^<(t) \\ &= \int \frac{d\omega'}{2\pi} e^{-i\omega't} \left( \langle bb^\dagger \rangle \int_0^\infty e^{i(\omega - \omega_0)t} \mathcal{G}_{00}^>(\omega') + \langle b^\dagger b \rangle \int_0^\infty e^{i(\omega + \omega_0)t} \mathcal{G}_{00}^>(\omega') \right. \\ &\quad \left. - \langle bb^\dagger \rangle \int_0^\infty e^{i(\omega + \omega_0)t} \mathcal{G}_{00}^<(\omega') - \langle b^\dagger b \rangle \int_0^\infty e^{i(\omega - \omega_0)t} \mathcal{G}_{00}^<(\omega') \right). \end{aligned} \quad (\text{A30})$$

Therefore, upon carrying out the time-integrations, we obtain

$$\begin{aligned} G_{0Q0Q}^{r(a)}(\omega) &= i \int \frac{d\omega'}{2\pi} \left\{ \mathcal{G}_{00}^>(\omega') \left( \frac{\langle bb^\dagger \rangle}{\omega - \omega_0 - \omega' \pm i0^+} + \frac{\langle b^\dagger b \rangle}{\omega + \omega_0 - \omega' \pm i0^+} \right) \right. \\ &\quad \left. - \mathcal{G}_{00}^<(\omega') \left( \frac{\langle bb^\dagger \rangle}{\omega + \omega_0 - \omega' \pm i0^+} + \frac{\langle b^\dagger b \rangle}{\omega - \omega_0 - \omega' \pm i0^+} \right) \right\}. \end{aligned} \quad (\text{A31})$$

Similarly,

$$\begin{aligned} G_{0Q0Q}^<(\omega) &= i \int dt e^{i\omega t} \langle (b + b^\dagger)(b(t) + b^\dagger(t)) \rangle \langle c_0^\dagger c_0(t) \rangle \\ &= i \langle bb^\dagger \rangle \int dt e^{i(\omega + \omega_0)t} \langle c_0^\dagger c_0(t) \rangle + i \langle b^\dagger b \rangle \int dt e^{i(\omega - \omega_0)t} \langle c_0^\dagger c_0(t) \rangle, \end{aligned} \quad (\text{A32})$$

and consequently

$$\begin{aligned} G_{0Q0Q}^<(\omega) &= \langle b^\dagger b \rangle \mathcal{G}_{00}^<(\omega - \omega_0) + \langle bb^\dagger \rangle \mathcal{G}_{00}^<(\omega + \omega_0), \\ G_{0Q0Q}^>(\omega) &= \langle b^\dagger b \rangle \mathcal{G}_{00}^>(\omega + \omega_0) + \langle bb^\dagger \rangle \mathcal{G}_{00}^>(\omega - \omega_0), \end{aligned} \quad (\text{A33})$$

where  $\mathcal{G}_{00}$  is the Green function on the dot in the absence of the coupling with the oscillator, see Eqs. (A15). It is easy to check that at zero temperature and *at equilibrium*, Eq. (A32) reduces to the usual diagrammatic expression, see e.g., Ref. 44.

In order to present explicit expressions for the self-energy due to the harmonic oscillator, we use [see Eqs.

(A12) and (A15)]

$$\begin{aligned} \mathcal{G}_{00}^<(\omega) &= i |\mathcal{G}_{00}^r(\omega)|^2 \Gamma_0(\omega) (f_L(\omega) + f_R(\omega)), \\ \mathcal{G}_{00}^>(\omega) &= i |\mathcal{G}_{00}^r(\omega)|^2 \Gamma_0(\omega) (f_L(\omega) + f_R(\omega) - 2), \end{aligned} \quad (\text{A34})$$

where we have denoted

$$\Gamma_0(\omega) = \frac{\Sigma_0^a(\omega) - \Sigma_0^r(\omega)}{2i}. \quad (\text{A35})$$

It follows that [see Eqs. (A24) and (A31)]

$$\begin{aligned} \Sigma_{\text{ho}}^a(\omega) &= \gamma^2 \int \frac{d\omega'}{2\pi} |\mathcal{G}_{00}^r(\omega')|^2 \Gamma_0(\omega') \left( \frac{\langle bb^\dagger \rangle (2 - f_L(\omega') - f_R(\omega')) + \langle b^\dagger b \rangle (f_L(\omega') + f_R(\omega'))}{\omega - \omega_0 - \omega' \pm i0^+} \right. \\ &\quad \left. + \frac{\langle b^\dagger b \rangle (2 - f_L(\omega') - f_R(\omega')) + \langle bb^\dagger \rangle (f_L(\omega') + f_R(\omega'))}{\omega + \omega_0 - \omega' \pm i0^+} \right). \end{aligned} \quad (\text{A36})$$

It is instructive to interpret Eq. (A36) in the simple equilibrium case where  $f_L(\omega') = f_R(\omega') = f(\omega')$  as the change, within second-order perturbation theory in  $\gamma$ , of the energy of an electronic state at energy  $\omega$ , due to all other states, at a running energy  $\omega'$ . The term  $|\mathcal{G}_{00}^r(\omega')|^2 \Gamma_0(\omega')$  appearing before the large brackets is just the density of the latter states at zero-order in  $\gamma$ . For the imaginary part of  $\Sigma_{\text{ho}}^{r(a)}(\omega)$ , the first term in the large brackets is due to real transitions occurring by exciting the oscillator (intensity proportional to  $\langle bb^\dagger \rangle$ ) and going to  $\omega' = \omega - \omega_0$  with the blocking factor  $1 - f(\omega')$ , or

by absorbing a ‘phonon’ (intensity proportional to  $\langle b^\dagger b \rangle$ ) and going to  $\omega$  from the same  $\omega'$ , now with an initial population  $f(\omega')$ . The real part of  $\Sigma_{\text{ho}}^{r(a)}(\omega)$ , given by the principal part of the integrals, is just the corresponding perturbation-theory energy shift. Obviously, these real and imaginary parts satisfy the Kramers-Kronig relationships. The second term in the large brackets is likewise understood as involving transitions to the state  $\omega' = \omega + \omega_0$  (for the imaginary part) or to the states around it (for the real part).

\* Electronic address: oraentin@bgu.ac.il; Also at Tel Aviv University, Tel Aviv 69978, Israel

† Also at Tel Aviv University, Tel Aviv 69978, Israel

<sup>1</sup> M. A. Reed, C. Zhou, C. J. Muller, T. P. Burgin, and J. M. Tour, *Science* **278**, 252 (1997); J. Chen, M. A. Reed, A. M. Rawlett, and J. M. Tour, *ibid* **286**, 1550 (1999).

<sup>2</sup> J. Reichert, R. Ochs, D. Beckmann, H. B. Weber, M. Mayor, and H. v. Lohneysen, *Phys. Rev. Lett.* **88**, 176804 (2002).

<sup>3</sup> N. B. Zhitenev, H. Meng, and Z. Bao, *Phys. Rev. Lett.* **88**, 226801 (2002).

<sup>4</sup> S. Kubatkin, A. Danilov, M. Hjort, J. Cornil, J. Bredas, N. Stuhr-Hansen, P. Hedegard, and T. Bjornholm, *Nature (London)* **425**, 698 (2003).

<sup>5</sup> J. G. Kushmerick, J. Lazorcik, C. H. Patterson, R. Shashidhar, D. S. Seferos, and G. C. Bazan, *Nano Lett.* **4**, 639 (2004).

<sup>6</sup> X. H. Qiu, G. V. Nazin, and W. Ho, *Phys. Rev. Lett.* **92**,

- 206102 (2004).
- <sup>7</sup> H. Park, J. Park, A. K. L. Lim, E. H. Anderson, A. P. Alivisatos, and P. L. McEuen, *Nature (London)* **407**, 57 (2000); A. N. Pasupathy, J. Park, C. Chang, A. V. Soldatov, S. Lebedkin, R. C. Bialczak, J. E. Grose, L. A. K. Donev, J. P. Sethna, D. C. Ralph, and P. L. McEuen, *Nano Lett.* **5**, 203 (2005).
  - <sup>8</sup> B. J. LeRoy, S. G. Lemay, J. Kong, and C. Dekker, *Nature (London)* **432**, 371 (2004).
  - <sup>9</sup> R. H. M. Smit, Y. Noat, C. Untiedt, N. D. Lang, M. C. van Hemert, and J. M. van Ruitenbeek, *Nature (London)* **419**, 906 (2002); D. Djukic, K. S. Thygesen, C. Untiedt, R. H. M. Smit, K. W. Jacobsen, and J. M. van Ruitenbeek, *Phys. Rev. B* **71**, 161402 (2005); W. H. A. Thijssen, D. Djukic, A. F. Otte, R. H. Bremmer, and J. M. van Ruitenbeek, *Phys. Rev. Lett.* **97**, 226806 (2006).
  - <sup>10</sup> O. Tal, M. Krieger, B. Leerink, and J. M. van Ruitenbeek, *Phys. Rev. Lett.* **100**, 196804 (2008); M. Kiguchi, O. Tal, S. Wohlthat, F. Pauly, M. Krieger, D. Djukic, J. C. Cuevas, and J. M. van Ruitenbeek, *Phys. Rev. Lett.* **101**, 046801 (2008).
  - <sup>11</sup> A. Aviram and M. A. Ratner, *Chem. Phys. Lett.* **29**, 277 (1974).
  - <sup>12</sup> A. Zazunov, A. Schulz, and R. Egger, *Phys. Rev. Lett.* **102**, 047002 (2009).
  - <sup>13</sup> J. Gaudioso, L. J. Lauhon, and W. Ho, *Phys. Rev. Lett.* **85**, 1918 (2000).
  - <sup>14</sup> B. Y. Choi, S. J. Kahng, S. Kim, H. Kim, H. W. Kim, Y. J. Song, J. Ihm, and Y. Kuk, *Phys. Rev. Lett.* **96**, 156106 (2006).
  - <sup>15</sup> J. Kirtley, D. J. Scalapino, and P. K. Hansma, *Phys. Rev. B* **14**, 3177 (1976).
  - <sup>16</sup> A. Mitra, I. Aleiner, and A. J. Millis, *Phys. Rev. B* **69**, 245302 (2004); *Phys. Rev. Lett.* **94**, 076404 (2005).
  - <sup>17</sup> T. Holstein, *Ann. Phys.* **8**, 325 (1959).
  - <sup>18</sup> V. Aji, J. E. Moore, and C. M. Varma, *Int. J. Nano.* **3**, 255 (2004).
  - <sup>19</sup> J. Koch and F. von Oppen, *Phys. Rev. Lett.* **94**, 206804 (2005).
  - <sup>20</sup> L. Glazman and R. I. Shekhter, *Zh. Eksp. Teor. Fiz.* **94**, 292 (1987) [*Sov. Phys. JETP* **67**, 163 (1988)].
  - <sup>21</sup> N. S. Wingreen, K. W. Jacobsen, and J. W. Wilkins, *Phys. Rev. B* **40**, 11834 (1989).
  - <sup>22</sup> K. Flensberg, *Phys. Rev. B* **68**, 205323 (2003).
  - <sup>23</sup> M. Čížek, M. Thoss, and W. Domcke, *Phys. Rev. B* **70**, 125406 (2004).
  - <sup>24</sup> U. Lundin and H. McKenzie, *Phys. Rev. B* **66**, 075303 (2002).
  - <sup>25</sup> J.-X. Zhu and A. V. Balatsky, *Phys. Rev. B* **67**, 165326 (2003).
  - <sup>26</sup> S. Bandopadhyay and D. Cohen, *Phys. Rev. B* **77**, 155438 (2008).
  - <sup>27</sup> T. L. Schmidt and A. Komnik, arXiv:0903.0916; R. Avriller and A. Levy Yeyati, arXiv:0903.0939; F. Haupt, T. Novotny, and W. Belzig, arXiv:0903.2268.
  - <sup>28</sup> K. D. McCarthy, N. Prokof'ev, and M. T. Tuominen, *Phys. Rev. B* **67**, 245415 (2003).
  - <sup>29</sup> M. Galperin, M. A. Ratner, and A. Nitzan, *J. Chem. Phys.* **121**, 11965 (2004); *J. Phys.: Condens. Matter* **19**, 103201 (2007).
  - <sup>30</sup> R. Härtle, C. Benesch, and M. Thoss, *Phys. Rev. Lett.* **102**, 146801 (2009).
  - <sup>31</sup> J. K. Viljas, J. C. Cuevas, F. Pauly, and M. Häfner, *Phys. Rev. B* **72**, 245415 (2005).
  - <sup>32</sup> D. A. Ryndyk, M. Hartung, and G. Cuniberti, *Phys. Rev. B* **73**, 045420 (2006).
  - <sup>33</sup> M. Paulsson, T. Frederiksen, and M. Brandbyge, *Phys. Rev. B* **72**, 201101 (2005); T. Frederiksen, N. Lorente, M. Paulsson, and M. Brandbyge, *ibid.* **75**, 235441 (2007).
  - <sup>34</sup> L. de la Vega, A. Martin-Rodero, N. Agrait, and A. Levy Yeyati, *Phys. Rev. B* **73**, 075428 (2006).
  - <sup>35</sup> R. Egger and A. O. Gogolin, *Phys. Rev. B* **77**, 113405 (2008).
  - <sup>36</sup> D. Fedorets, L. Y. Gorelik, R. I. Shekhter, and M. Jonson, *Europhys. Lett.* **58**, 99 (2002).
  - <sup>37</sup> J. Koch, M. Semmelhack, F. von Oppen, and A. Nitzan, *Phys. Rev. B* **73**, 155306 (2006).
  - <sup>38</sup> S. Engelsberg and J. R. Schrieffer, *Phys. Rev.* **131**, 993 (1963).
  - <sup>39</sup> Y. Meir and N. Wingreen, *Phys. Rev. Lett.* **68**, 2512 (1992).
  - <sup>40</sup> See e.g. Y. Imry and R. Landauer, *Rev. Mod. Phys.* **71**, S306 (1999).
  - <sup>41</sup> In Ref. 35, the part of the current arising from the real part of  $\Sigma_{ho}$  is termed 'quasielastic', while the one involving the imaginary part is called 'inelastic'.
  - <sup>42</sup> Note that contrary to our Fig. 2, Fig. 11 of Ref. 16 shows that the conductance in the presence of the coupling with the harmonic oscillator is always *larger* than the one in the absence of that coupling.
  - <sup>43</sup> L. V. Keldysh, *Sov. Phys. JETP* **20**, 1018 (1965); D. C. Langreth, in *Linear and Nonlinear Electron Transport in Solids*, Vol. 17 of Nato Advanced Study Institute, Series B: Physics, edited by J. T. Devreese and V. E. Van Doren (Plenum, New York, 1976).
  - <sup>44</sup> A. Martin-Rodero, A. Levy Yeyati, F. Flores, and R. C. Monreal, arXiv0811.4531.